

# 2D and 3D Hybrid Systems for Enhancement of Chondrogenic Differentiation of Tonsil-Derived Mesenchymal Stem Cells

Jinhye Park, In Young Kim, Madhumita Patel, Hyo Jung Moon, Seong-Ju Hwang, and Byeongmoon Jeong\*

2D/3D hybrid cell culture systems are constructed by increasing the temperature of the thermogelling poly(ethylene glycol)-poly(L-alanine) diblock copolymer (PEG-L-PA) aqueous solution in which tonsil tissue-derived mesenchymal stem cells and graphene oxide (GO) or reduced graphene oxide (rGO) are suspended, to 37 °C. The cells exhibit spherical cell morphologies in 2D/3D hybrid culture systems of GO/PEG-L-PA and rGO/PEG-L-PA by using the growth medium. The cell proliferations are 30%–50% higher in the rGO/PEG-L-PA hybrid system than in the GO/PEG-L-PA hybrid system. When chondrogenic culture media enriched with TGF- $\beta$ 3 is used in the 2D/3D hybrid systems, cells extensively aggregate, and the expression of chondrogenic biomarkers of SOX 9, COL II A1, COL II, and COL X significantly increases in the GO/PEG-L-PA 2D/3D hybrid system as compared with the PEG-L-PA 3D systems and rGO/PEG-L-PA 2D/3D hybrid system, suggesting that the GO/PEG-L-PA 2D/3D hybrid system can be an excellent candidate as a chondrogenic differentiation platform of the stem cell. This paper also suggests that a 2D/3D hybrid system prepared by incorporating 2D materials with various surface biofunctionalities in the in situ forming 3D hydrogel matrix can be a new cell culture system.

## 1. Introduction

Control of stem cell differentiation into a specific cell type is the most important step for successful stem cell therapy. Otherwise, stem cells may differentiate into unwanted cells or tissues, and can sometimes lead to the development of tumors.<sup>[1,2]</sup> The biochemical factors and materials parameters of scaffolds are the main areas of the research on stem cell differentiation.<sup>[3–5]</sup> Many biochemical factors including dexamethasone, ascorbic acid, and various growth factors have been developed.<sup>[6,7]</sup> Also, physicochemical parameters of scaffolds such as topography, mechanical properties, roughness of substrates, and chemical or biochemical functional groups have been reported to control

stem cell differentiation.<sup>[8–11]</sup> The focal adhesion of stem cells to a matrix scaffold and biochemical signaling cascades were suggested to be responsible for the differentiation of stem cells by the above parameters.<sup>[12,13]</sup>

Recent studies also demonstrated that dimensional control of a material such as 1D fibers, 2D sheets, and 3D hydrogels is very important for stem cell differentiation.<sup>[14–16]</sup> Orientation, length, and diameter of nanofibers affect the stem cell differentiation and the 1D materials were reported to be particularly effective in directing the neuronal differentiation of stem cells.<sup>[15,16]</sup> Traditionally, cell cultures have been studied using the 2D system of polystyrene plate. However, the cells cultured in 3D culture systems exhibited biomarker expressions and phenotypes different from the cells cultured on 2D systems.<sup>[17,18]</sup> As a 2D surface, graphene (G) or reduced graphene oxide (rGO) and graphene oxide (GO) have recently

been investigated for cell and stem cell culture.<sup>[19,20]</sup> G and GO with different surface functional groups, were reported to be effective in inducing osteogenesis and adipogenesis, respectively.<sup>[19,20]</sup> The interactions between G or GO surfaces and proteins in the culture media were claimed to be responsible for the different behaviors. More recently, when transforming growth factor beta 3 (TGF- $\beta$ 3) and fibronectin adsorbed on GO were incorporated into the pellets of adipose-derived stem cells, enhancement of chondrogenesis was observed.<sup>[21]</sup>

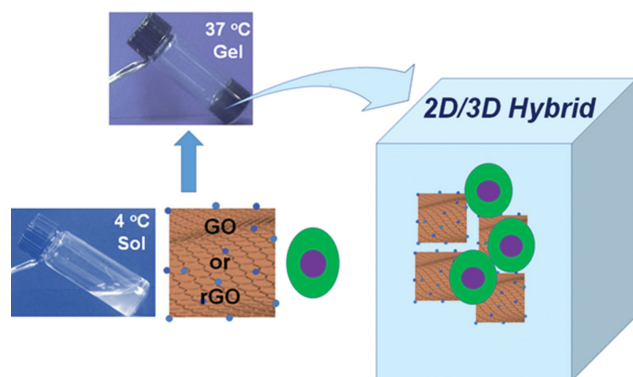
Thermogelling polymer aqueous solutions undergo sol-to-gel transition as the temperature increases. Cells or stem cells can be incorporated in an in situ formed gel by heating an aqueous solution of the cells or stem cells in a sol state into a warm environment, typically 37 °C. Due to the simple procedure and mild conditions for hydrogel formation, thermogelling polymers have been applied for 3D cell cultures and injectable tissue engineering.<sup>[22–25]</sup>

In our current study, we designed a 2D/3D hybrid system for the culture of tonsil-derived mesenchymal stem cells (TMSCs). TMSCs are isolated from human palatine tonsils which can be easily obtained from otherwise waste tissues of tonsils after a tonsillectomy.<sup>[26,27]</sup> In particular, the population density of the MSCs from the tonsil is greater, and the proliferation rate of

J. Park, I. Y. Kim, Dr. M. Patel, H. J. Moon, Prof. S.-J. Hwang, Prof. B. Jeong  
Department of Chemistry and Nano Science  
Ewha Global Top 5 Research Program  
Ewha Womans University  
52 Ewhayodae-gil, Seodaemun-gu  
Seoul 120-750, South Korea  
E-mail: bjeong@ewha.ac.kr



DOI: 10.1002/adfm.201500299



**Scheme 1.** Preparation of the 2D/3D hybrid culture system for TMSCs. TMSCs suspended in PEG-L-PA aqueous solution containing GO or rGO were heated to a cell culture temperature of 37 °C, where heat-induced in situ gel formation leads to the 2D/3D hybrid cell culture system.

the TMSCs is greater is faster, compared with those of bone marrow derived MSCs.<sup>[27–29]</sup> Recently, favorable chimerism from several donors was reported, therefore TMSCs can be mixed without a significant loss of their stem cell properties.<sup>[30]</sup> With the above advantages as a resource of MSCs, more intensive studies should be explored urgently on the TMSCs.

The poly(ethylene glycol)-poly(L-alanine) diblock copolymer (PEG-L-PA) aqueous solution undergoing temperature-sensitive sol-to-gel transition was used for in situ preparation of a hydrogel, where GO or rGO was coencapsulated with TMSCs in the hydrogel during the sol-to-gel transition (Scheme 1). Thus, 2D/3D hybrid cell culture systems consisting of GO or rGO dispersed hydrogel were prepared. The in situ formed hydrogel provided the 3D matrix, where the encapsulated GO or rGO provided the 2D surfaces. The characteristic cell morphology, and mRNA and protein expressions related to stem differentiation in 2D/3D hybrid systems were investigated. As control experiments, TMSCs were 2D cultured on the GO and rGO surface and were 3D cultured in the PEG-L-PA thermogel.

## 2. Results and Discussion

Thermogelling polymer of PEG-L-PA was synthesized by ring-opening polymerization of N-carboxy anhydride of L-alanine in the presence of  $\alpha$ -amino- $\omega$ -methoxy PEG.<sup>[25]</sup> Based on the methyl peak of PA at 1.40–1.90 ppm (internal methyl group at 1.40–1.70 ppm and terminal methyl group at 1.70–1.90) and the ethylene glycol peak of PEG at 3.80–4.20 ppm in the <sup>1</sup>H-NMR spectra of the PEG-L-PA, the molecular weights ( $M_n$ ) of each block of PEG-L-PA was calculated to be 1000–970 Da (Figure S1a, Supporting Information). The molecular weight ( $M_n$ ) and the molecular weight distribution determined by gel permeation chromatography (GPC) relative to PEG standards were 1120 Da and 1.1, respectively (Figure S1b, Supporting Information). As the concentration increased from 0.001 to 1.0 wt%, the CD band shifted to a longer wavelength at 220–230 nm, and the band shape became narrow (Figure S1c, Supporting Information). The increase in the band intensity at 220–230 nm is an indication of self-assemblies of the PEG-L-PA.<sup>[24,31–33]</sup> Similar changes in peak shape and red-shift of the peak were observed as the

temperature increased from 10 to 60 °C, thereby suggesting that the aggregation or assembly of the polymer occurred as the temperature increased (Figure S1d, Supporting Information). <sup>1</sup>H-NMR spectrum of PEG-L-PA (5.5 wt% in D<sub>2</sub>O) exhibited that shifts and broadening of PEG peak, as the temperature increased from 10 to 60 °C (Figure S1e, Supporting Information), suggesting that PEG dehydrated as the temperature increased.<sup>[34–36]</sup> Based on the CD and <sup>1</sup>H-NMR spectra, the dehydration and aggregation of PEG-L-PA are involved in the sol-to-gel transition of the polymer aqueous solution.

The 2D nanosheets of monolayer flakes of GO and rGO that were several micrometers in size were prepared as shown in the transmission electron microscopy (TEM) images (Figure 1a). The nature of chemical bonding of the GO and rGO nanosheets was examined by micro-Raman spectroscopy and x-ray photoelectron spectroscopy (XPS). The characteristic D band and G band in the Raman spectra were shown at 1366 and 1606 cm<sup>−1</sup> for GO whereas they were shown at 1363 and 1604 cm<sup>−1</sup> for rGO, respectively. The D band is related to the defect-induced breathing mode of sp<sup>2</sup> rings and comes from the C–C stretching mode of sp<sup>2</sup> carbons whereas the G band comes from the first order scattering of the E<sub>2g</sub> phonon of sp<sup>2</sup> carbon atoms.<sup>[37]</sup> The area ratio of the D band to the G band ( $A_D/A_G$ ) of the Raman spectra is a measure of disorder degree and inversely proportional to the size of the sp<sup>2</sup> domain.<sup>[38]</sup>  $A_D/A_G$  measured by linear baseline between 1200 and 1700 cm<sup>−1</sup> was 1.23 and 1.51 for GO and rGO, respectively, thereby suggesting that the sp<sup>2</sup> domain cluster partially decreased after the reduction process of GO to rGO (Figure 1b). C1s XPS spectra of G and GO suggested that the surface carbon–oxygen bonds coming from C–OH, C–O–C, C=O, and O–C=O groups observed at 285–290 eV were significantly reduced after the reduction process of GO to rGO by hydrazine. (Figure 1c,d). The curve fitting results indicated that the ratio of the oxygen species of C–OH, C–O–C, C=O, and O–C=O groups to C–C groups decreased from 1.32 to 0.55 during the reduction process (Table 1).

The moduli of the polymer aqueous systems (5.5 wt%) in sol (4 °C) and gel (37 °C) states were compared by the dynamic mechanical analysis (Figure 2a). The polymer aqueous solution at 5.5 wt% was selected to provide a rather stiff gel with the modulus of 680 Pa at 37 °C. The storage modulus ( $G'$ ) and loss modulus ( $G''$ ) are measures of the elastic component and the viscous component of a complex modulus ( $G^*$ ), respectively.<sup>[39]</sup>  $G''$  was greater than  $G'$  at 4 °C whereas  $G'$  was greater than  $G''$  at 37 °C, indicating that the sol state at 4 °C turned into a gel state at 37 °C. The addition of GO or rGO to the polymer aqueous solution decreased the gel modulus at 37 °C. As the concentration of GO increased from 0.0 → 0.01 → 0.1 → 1.0 wt%, the gel modulus of the GO/PEG-L-PA hybrid system at 37 °C decreased from 680 → 610 → 470 → 330 Pa (Figure 2b). In contrast, the gel modulus of the rGO/PEG-L-PA hybrid system at 37 °C decreased from 680 → 630 → 580 → 500 Pa as the concentration of rGO increased from 0.0 → 0.01 → 0.1 → 1.0 wt% (Figure 2c). The hydrophilic surface property of GO more seriously decreased the modulus of the PEG-L-PA thermogel than the rGO with hydrophobic surfaces.  $G'$  greater than 300 Pa at 37 °C was good enough to hold the TMSCs during the cell culture, as would be discussed in cell culture section. The decrease in gel modulus by adding the GO

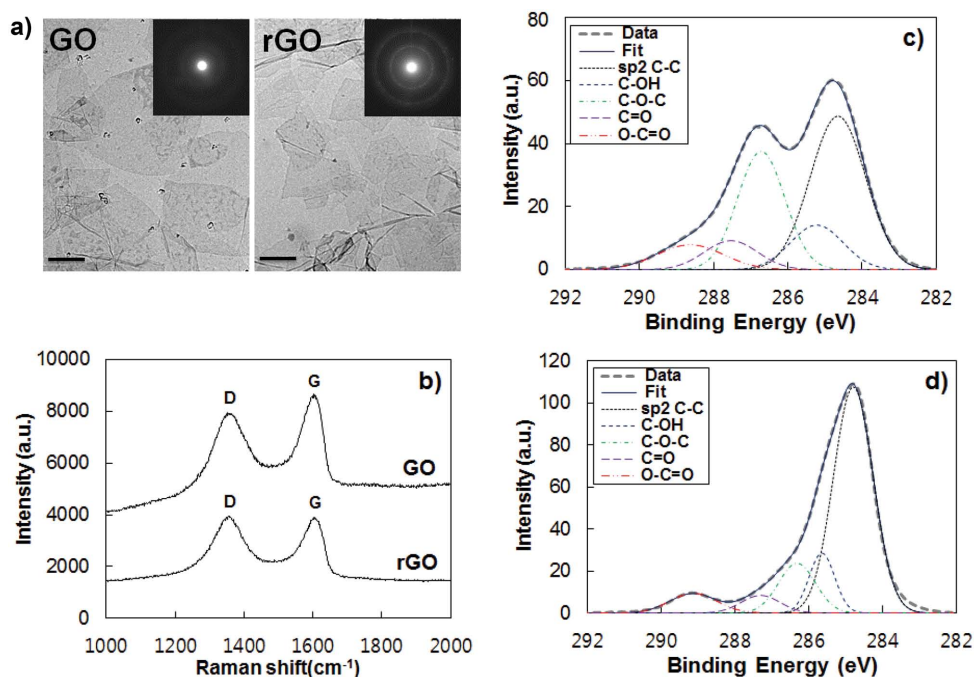


**Figure 1.** a) TEM images of GO and rGO. The scale bar is 1.0 μm. b) Raman spectra of GO and rGO. c) C1s XPS spectrum of GO. d) C1s XPS spectrum of rGO.

or rGO into PEG-L-PA aqueous system is related to the interactions between GO or rGO and PEG-L-PA as well as the water. CD spectra and FTIR spectra of the PEG-L-PA, GO/PEG-L-PA hybrid system, rGO/PEG-L-PA hybrid system suggested that the addition of GO or rGO into the PEG-L-PA aqueous solution slightly changed the secondary structure of L-PA (Figure S2, Supporting Information).

The photographs of the PEG-L-PA, GO/PEG-L-PA (G-1.0), and rGO/PEG-L-PA (GO-1.0) in sol state (4 °C) and gel state (37 °C) are shown (Figure 2d). GO-1.0 and rGO-1.0 are the hybrid systems prepared from GO (1.0 wt%)/PEG-L-PA (5.5 wt%) and rGO (1.0 wt%)/PEG-L-PA (5.5 wt%), respectively.

When the TMSCs were cultured on the 2D surfaces of GO and rGO by using the growth medium of Dulbecco's modified eagle medium (DMEM), the cell developed fibroblastic morphology and the cell population increased significantly in 14 days (Figure S3, Supporting Information). However, the expression of typical mesodermal differentiation biomarkers such as OCN, COL II, and PPAR $\gamma$  were negligible (Figure S4, Supporting Information). These facts indicated that both GO

and rGO provided good adhesion surfaces for TMSCs and the stem cells did not actively differentiate into the primary cells during the 2D culture.

2D/3D hybrid systems were prepared by increasing the temperature to 37 °C for TMSC-suspended PEG-L-PA aqueous solution (5.5 wt%) containing GO or rGO in a concentration range of 0.0–1.0 wt%. Considering the solid content of less than 6.5% in current study, the remaining part of the gel are filled with water, therefore the porosity of the gel is more than 93.5%. The pores act as channels for mass transport for metabolites and nutrients as well as cell migration during the 3D cell culture. A 3D culture system of PEG-L-PA was also prepared in the absence of GO or rGO for comparison. When the TMSCs were cultured in the 2D/3D hybrid systems of GO/PEG-L-PA or rGO/PEG-L-PA by using the growth medium of DMEM, the cells maintained spherical morphology, as would be discussed in Section 3. The population of the cell increased 2–4 times over 14 days (Figure 3a,b). The increase in cell population was greater in the rGO/PEG-L-PA hybrid system than the GO/PEG-L-PA hybrid system. In particular, the rGO in rGO/PEG-L-PA 2D/3D hybrid system in a concentration range of 0.01–0.1 wt% was effective in increasing the cell population compared with the 3D system of PEG-L-PA without rGO. We already reported the preferential chondrogenic differentiation of mesenchymal stem cell in the 3D culture system of PEG–polypeptide thermogels.<sup>[24,40]</sup> In our current study, among the above mesodermal biomarkers of OCN, COL II, and PPAR $\gamma$ , the COL II was highly expressed in the 2D/3D hybrid systems as well as in the PEG-L-PA 3D system. In particular, the COL II expression increased by more than ten times in the 2D/3D hybrid systems than in the PEG-L-PA 3D thermogel system (Figure 4a,b). The greatest increase in

**Table 1.** C1s XPS spectral analysis of GO and rGO.

Functional group	GO	rGO
	Relative area [%]	Relative area [%]
sp <sup>2</sup> C—C	43.2	64.4
C—OH	11.9	10.9
C—O—C	28.5	13.1
C=O	7.9	5.0
O—C=O	8.5	6.6

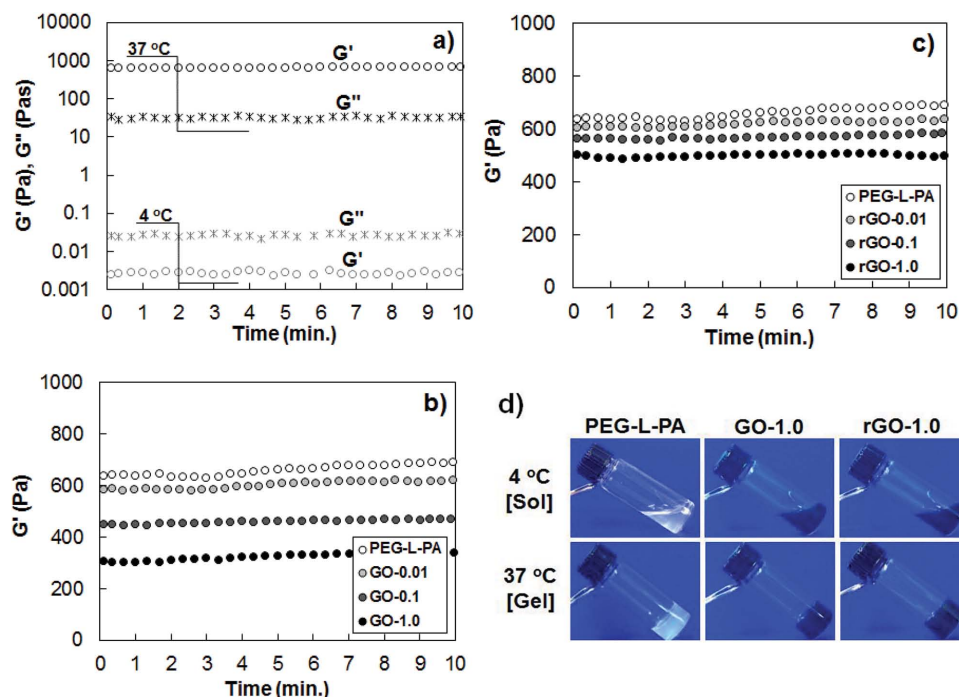


**Figure 2.** a) The storage modulus ( $G'$ ) and loss modulus ( $G''$ ) of PEG-L-PA aqueous solution (5.5 wt%) at sol (4 °C) and gel (37 °C) states. b) Storage modulus ( $G'$ ) of the GO/PEG-L-PA hybrid system at 37 °C as a function of GO concentration. c) Storage modulus ( $G'$ ) of the rGO/PEG-L-PA hybrid system at 37 °C as a function of rGO concentration. d) Photographs of the PEG-L-PA, GO/PEG-L-PA hybrid, and rGO/PEG-L-PA hybrid systems at 4 °C (sol) and 37 °C (gel). The numbers in the legend of GO-0.01, GO-0.1, GO-1.0, rGO-0.01, rGO-0.1, and rGO-1.0 indicate the concentration (wt%) of GO and rGO in the system, respectively.

COL II expression was observed in the GO/PEG-L-PA hybrid system containing 1.0 wt% of GO. Immunofluorescence analysis also indicated the same trend (Figure 5a,b). The COL II stained in red exhibited significantly high intensity in the GO/PEG-L-PA hybrid system. The semiquantitative analysis of the fluorescence image suggested that about ten times increase of COL II in the GO/PEG-L-PA hybrid system occurred, compared with the 3D system of PEG-L-PA thermogel (Figure 5c). Both real-time reverse transcription polymerase chain reactions (RT-PCR) and immunofluorescence studies indicated that 2D/3D hybrid systems prepared by GO and PEG-L-PA significantly improved the COL II expression in both mRNA and protein levels.

COL II is the major extracellular protein in articular cartilage and plays roles in differentiation, matrix remodeling, and mechanical stimulation. Chondrocytes bind to COL II ligands through  $\alpha 1\beta 1$ ,  $\alpha 2\beta 1$ , and  $\alpha 10\beta 1$  integrins, which affect the signaling cascade to chondrogenic differentiation and upregulate the chondrogenic genes such as SOX 9, COL II, and COL X.<sup>[41]</sup> COL II is also reported to enhance the chondrogenesis synergistically in the presence of TGF- $\beta 3$ .<sup>[41,42]</sup> TGF- $\beta 3$  is known to induce the chondrogenesis through the heterodimer complex formation and affect signaling cascades of the chondrogenic transcription mechanism.<sup>[43]</sup> Based on these reports and excellent COL II expression in the 2D/3D hybrid system, we designed a chondrogenic culture system for TMSCs in the 2D/3D hybrid systems prepared from 1.0 wt% of GO or rGO suspended PEG-L-PA aqueous solution, where the chondrogenic induction media enriched with TGF- $\beta 3$  was used. Live and dead

assay exhibited an excellent cell viability during the cell culture period with the live cells and dead cells stained as green and red, respectively. When the TMSCs were cultured by using growth media, fibroblast-like cell morphologies were observed during the 2D culture on GO and rGO whereas they changed into spherical shapes with some spindle-like extrusion during the culture in the 2D/3D hybrid systems of GO/PEG-L-PA or rGO/PEG-L-PA (Figure 6). On the other hand, an extensive aggregation of cells was observed in the 2D/3D hybrid systems when the TMSCs were cultured by using chondrogenic induction media, which was pronounced in the GO/PEG-L-PA hybrid system (Figure 6 bottom and Figure S5, Supporting Information). When the TMSCs were cultured in the 3D systems of PEG-L-PA, they exhibited spherical shape with little aggregation of the cells in both growth media and chondrogenic induction media (Figure S6, Supporting Information). The mRNA expression was studied for chondrogenic biomarkers of SOX 9, COL II A1, COL II, and COL X. Compared with the 3D system of PEG-L-PA thermogel, the cells expressed higher amounts of the above chondrogenic biomarkers in the 2D/3D hybrid system. SOX 9, COL II A1, and COL X mRNA expressions increased more than 2 times, 3–4 times, and 6–8 times, respectively, in the 2D/3D hybrid systems than in the PEG-L-PA 3D system (Figure 7a,b). In particular, the COL II mRNA expression increased 13 times higher in the GO/PEG-L-PA hybrid system than in the PEG-L-PA 3D system (Figure 7b). Immunofluorescence study also confirmed the chondrogenic differentiation of the TMSCs in the 2D/3D hybrid system in the protein level (Figure 8a,b). Nucleus and actin were stained to blue and green



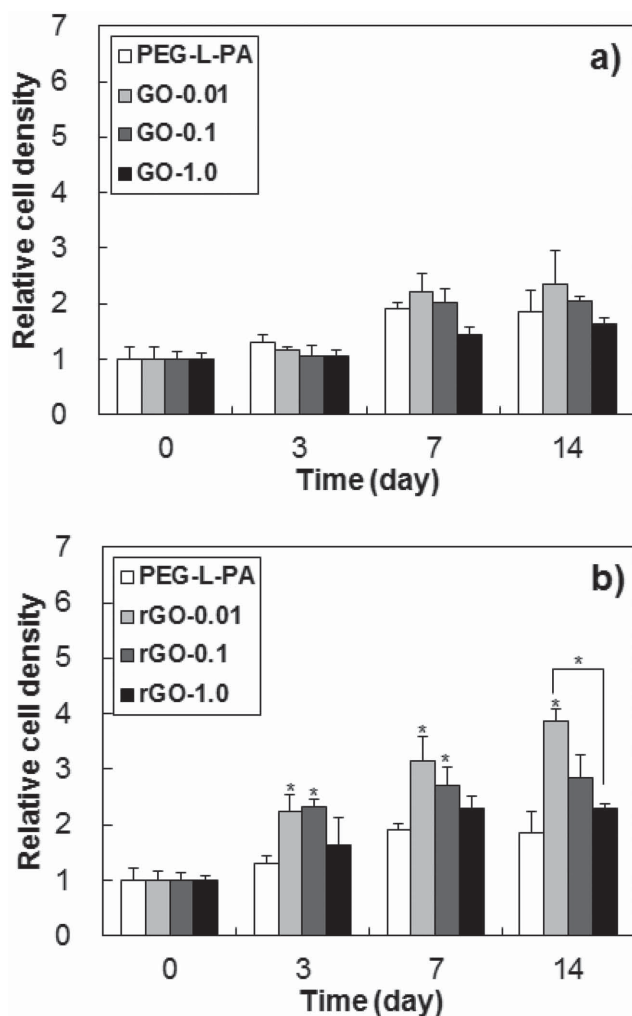


**Figure 3.** Change in cell density relative to the zeroth day in the a) GO/PEG-L-PA hybrid system and b) the rGO/PEG-L-PA hybrid system during the cell culture period. Growth media of DMEM was used for cell culture. The \* on the bar graph indicates the significance (\*:  $p < 0.05$ ) of the 2D/3D hybrid system compared with the PEG-L-PA 3D culture system.  $n = 3$ .

by 4',6'-diamidino-2-phenyl indole (DAPI) and phalloidin, respectively. SOX 9 and COL II which are typical proteins related to chondrogenesis were stained red by their corresponding antibodies. The immunofluorescence study also suggested that significant increases in COL II expression as well as cell aggregation occurred in the GO/PEG-L-PA hybrid system (Figure 8b). Semiquantitative analysis of the fluorescence images demonstrated that about a doubling in SOX 9 and ten times increase in COL II occurred in the GO/PEG-L-PA hybrid system as compared with the PEG-L-PA 3D thermogel system (Figure 8c).

Both RT-PCR and immunofluorescence studies suggested that chondrogenesis was significantly improved by 2D/3D hybrid system. The detailed mechanism on the enhancement of the chondrogenesis is open for further study. It is widely accepted that physicochemical factors play an important role in directing the differentiation of stem cells. In our current study, it was evident that the difference in surface functional

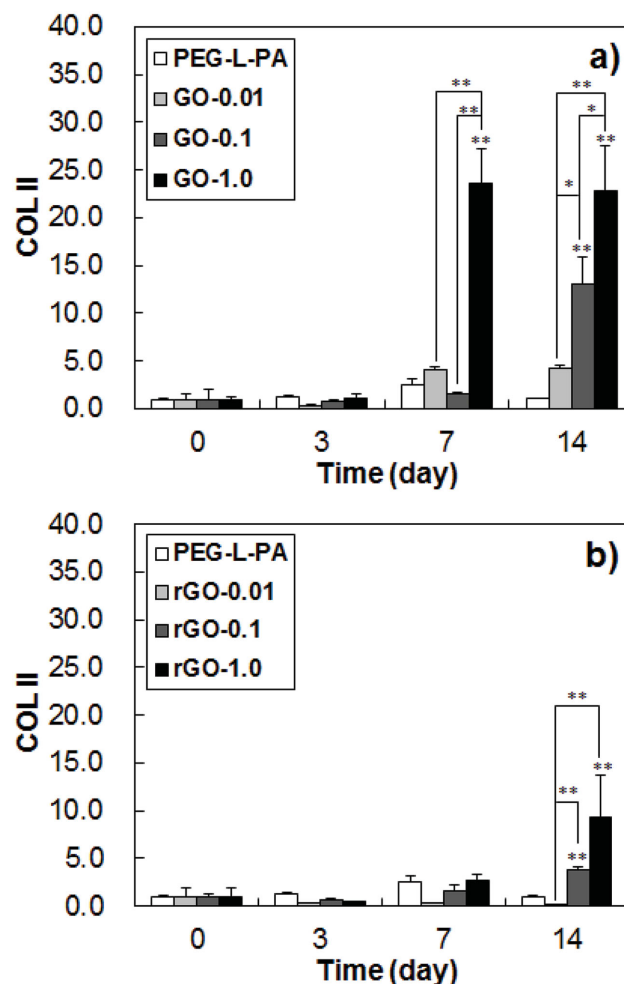


**Figure 4.** Comparison of mRNA expression of COL II during the TMSCs culture in the a) GO/PEG-L-PA hybrid system and b) the rGO/PEG-L-PA hybrid system as a function of GO and rGO concentration. Growth media of DMEM was used for cell culture. The data were normalized by the GAPDH and zeroth day. The data are presented as the mean  $\pm$  SD of three independent experiments ( $n = 3$ ). Zeroth day indicated 4 h after the 3D culture started. The \* or \*\* on the bar graph indicates the significance of the 2D/3D hybrid system compared with the PEG-L-PA 3D culture system.

groups between GO and rGO played a role. Recent studies by Anseth and co-workers reported that PEG hydrogel tethered with carboxylate groups, phosphate groups, and t-butyl groups significantly increased the chondrogenesis, osteogenesis, and adipogenesis, respectively, than unmodified PEG hydrogel.<sup>[11]</sup> We also reported that the surface-functionalized microspheres dispersed in the polypeptide thermogel also controlled the differentiation of the stem cells.<sup>[44]</sup> In particular, carboxylate modified polystyrene microspheres significantly enhanced the chondrogenesis compared to unmodified polystyrene microspheres in the 3D culture system. The recent research and our current study suggest that carboxylate functional groups might be effective in inducing chondrogenesis of stem cells. GO also has carboxylate and hydroxyl groups on the surface. The hydroxyl and carboxylate resemble the functional groups of glycosaminoglycan

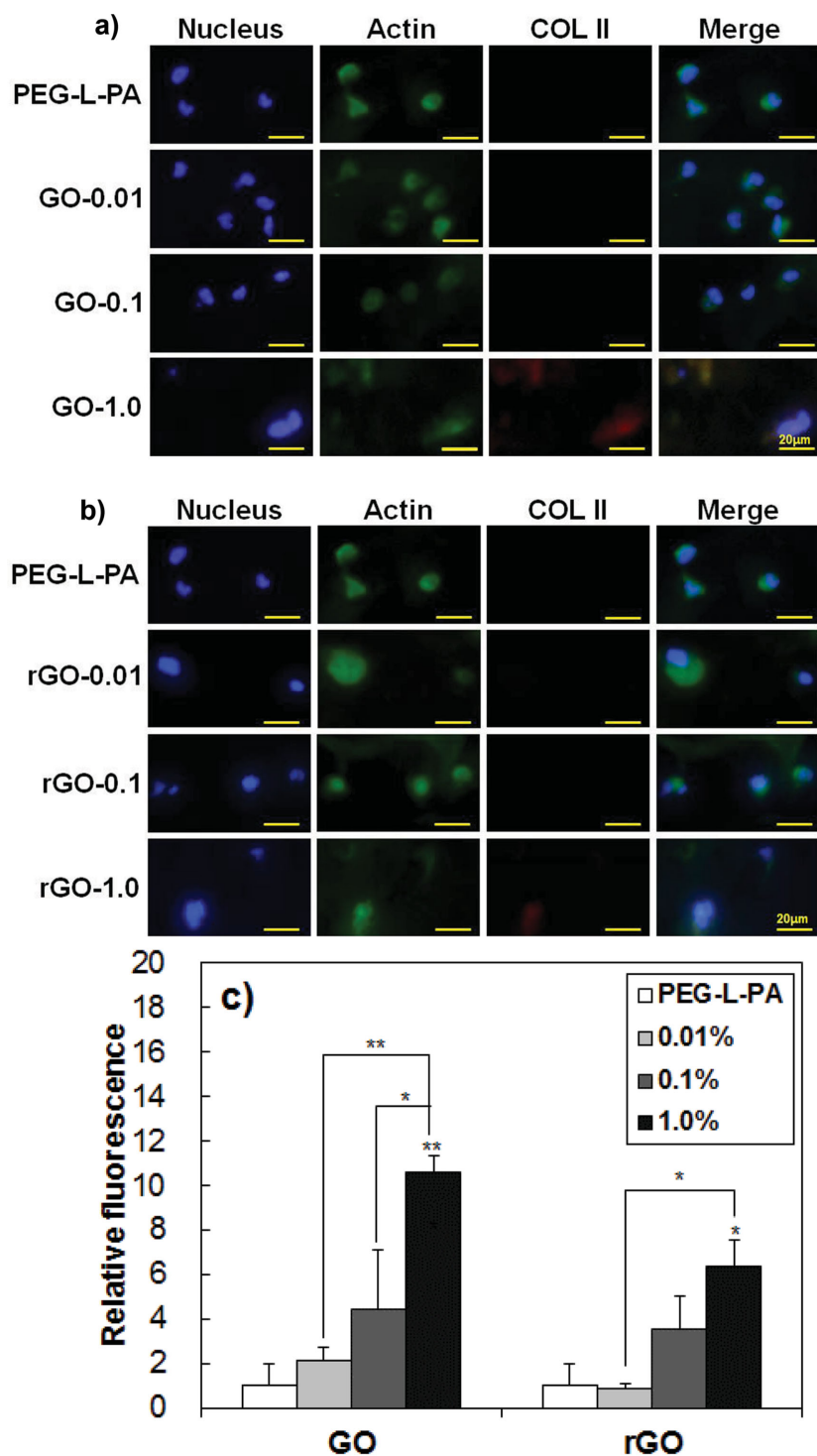


**Figure 5.** Immunofluorescence images for biomarker expressions during TMSC culture in a) the GO/PEG-L-PA system and b) the rGO/PEG-L-PA system as a function of GO or rGO concentration. The scale bar is 20  $\mu$ m. Growth media of DMEM was used for cell culture. Nucleus and actin were stained by DAPI and phalloidin, respectively. COL II was stained by corresponding antibodies. c) Semiquantification of the fluorescence images by the number of stained cell times fluorescence intensity. The \* or \*\* on the bar graph indicates the significance of the 2D/3D hybrid system compared with the PEG-L-PA 3D culture system.  $n = 3$ .

and hyaluronic acid which are components of the extracellular matrix of the native cartilage. Hyaluronic acid is reported to improve chondrocyte proliferation during the 3D culture.<sup>[45]</sup> In our current study, the chondrogenic media enriched with TGF  $\beta$ 3 was particularly effective in cell aggregation as well as chondrogenic differentiation. TGF  $\beta$ 3 binds to its receptor on the cell surface and directs the chondrogenic differentiation through the signaling cascade.<sup>[46]</sup> TGF  $\beta$ 3 can bind to GO through the balanced interactions between electrostatic and hydrophobic interactions.<sup>[21]</sup> TGF  $\beta$ 3 bound to GO could play a role in cell differentiation in a time-controlled manner. In addition, the specific functional group of GO might recruit other serum proteins to bind to the GO, and the proteins can cooperatively affect the signaling cascade for the chondrogenesis of the stem cells.<sup>[47]</sup> On the other hand, functional groups of GO might also direct cell–matrix interactions to induce tissue-specific matrix molecules, which might, in turn, affect stem cell differentiation.<sup>[48]</sup>

To summarize, TMSCs can be an excellent resource for chondrogenic cells and a 3D hybrid system incorporating 2D biocompatible materials with the appropriate surface functional groups can be a promising treatment for articular cartilage defects.

### 3. Conclusions

During the 2D culture of TMSCs, cells proliferated and developed fibroblast-like morphology on the GO and rGO, suggesting the GO and rGO provided good adhesion or interaction sites. The 2D/3D hybrid systems were prepared by heating the GO or rGO suspended PEG-L-PA aqueous solutions to 37  $^{\circ}$ C. There is no significant mesodermal differentiation on the 2D culture system. On the other hand, preferential expression of the chondrogenic differentiation biomarker of COL II was observed in the PEG-L-PA 3D system, while the COL II expression significantly increased in the 2D/3D hybrid culture systems of GO/PEG-L-PA and rGO/PEG-L-PA.

When a TGF- $\beta$ 3 enriched chondrogenic medium was used in the 2D/3D hybrid systems of GO/PEG-L-PA and rGO/PEG-L-PA, not only cell aggregation but also chondrogenic differentiation dramatically increased. In particular, the most significant increase in

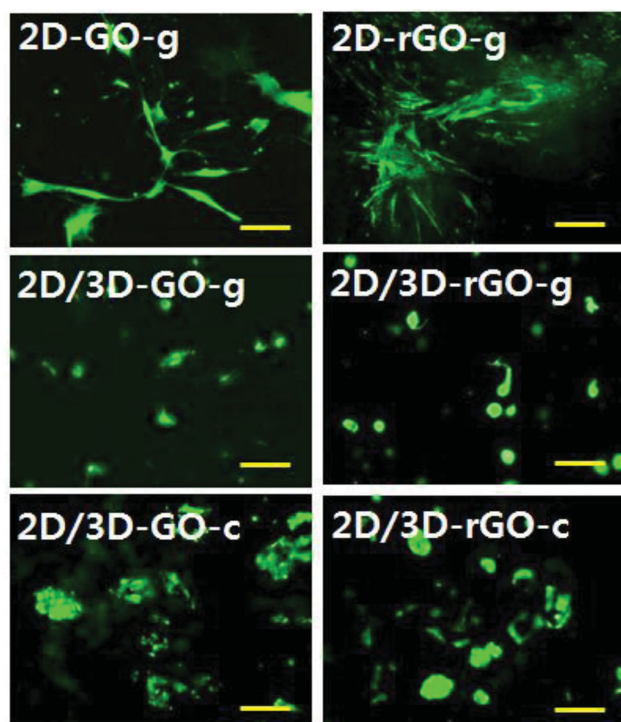


**Figure 6.** Change in cell morphology after 14 days of cell culture. Top: 2D culture on the GO (left) and rGO (right) by using the growth media of DMEM, middle; 3D culture in the GO/PEG-L-PA (left) and rGO/PEG-L-PA (right) hybrid gels using the growth media of DMEM, and bottom; 3D culture in the GO/PEG-L-PA (left) and rGO/PEG-L-PA (right) hybrid gels using chondrogenic induction media enriched with TGF- $\beta$ 3 in DMEM. The numbers in the legend of GO-1.0 and rGO-1.0 indicate the concentration (1.0 wt%) of GO and rGO, respectively, in the system. The scale bar is 100  $\mu$ m.

chondrogenic biomarker expression including SOX 9, COL II A1, COL II, and COL X were observed in the GO/PEG-L-PA 2D/3D hybrid system. The enhancement might be closely related to the cooperative interactions among TGF- $\beta$ 3, COL II, and GO for signaling cascades of the chondrogenic differentiation. GO might provide not only 2D surfaces for cell adhesion but also interaction sites between COL II and TGF- $\beta$ 3. In addition, GO increased the aggregation of the cells.

This paper proves that 1) cell morphology dramatically changes depending on the dimensions of the culture system and the medium composition; 2) COL II and TGF- $\beta$ 3 synergistically contribute to the chondrogenesis of stem cells; 3) a 2D/3D hybrid culture system in situ formed by thermogelation provides an effective method in controlling stem cell differentiation, where surface chemistry of incorporated 2D materials plays an important role in inducing expression of specific biomarkers. With a mild condition for gel formation and maintaining neutral pH during degradation, our polypeptide thermogelling system can provide an in situ forming 3D cell culture system. This paper also suggests a new 2D/3D hybrid system can be designed for controlling stem cell differentiation by incorporating 2D materials with various surface functional groups in the in situ forming 3D hydrogel matrix.

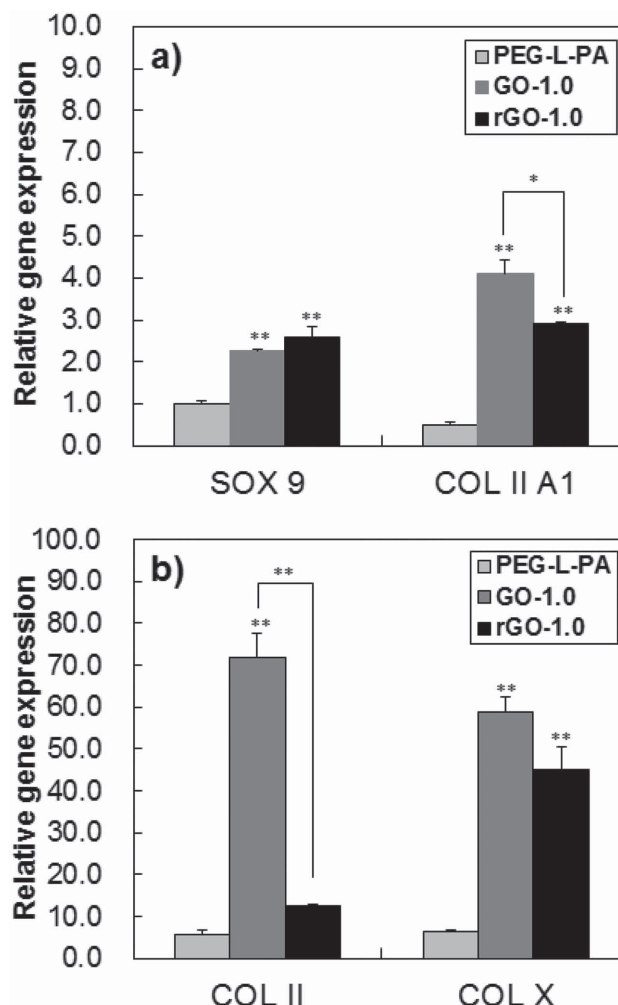


**Figure 7.** Comparison of chondrogenic mRNA expression during the TMSCs culture in the PEG-L-PA, GO/PEG-L-PA hybrid, and rGO/PEG-L-PA hybrid systems. Chondrogenic induction media enriched with TGF- $\beta$ 3 was used for cell culture. SOX 9, COL II A1, COL II, and COL X were compared. The data were normalized by the GAPDH and zeroth day. The data are presented as the mean  $\pm$  SD of three independent experiments ( $n = 3$ ). The \* or \*\* on the bar graph indicates the significance of the 2D/3D hybrid system compared with the PEG-L-PA 3D culture system.

#### 4. Experimental Section

**Materials:**  $\alpha$ -amino- $\omega$ -methoxy PEG (MW = 1000 Da, IDB Chem, Korea) and N-carboxy anhydrides of L-alanine (KPX life, Korea) were used as received. Chloroform was dried over magnesium sulfate before use. Anhydrous N,N-dimethyl form amide was used as received from Sigma-Aldrich (USA). Toluene (Daejung, Korea) was distilled over sodium before use. The aqueous colloidal suspension of exfoliated GO nanosheets was synthesized by the modified Hummers' method.<sup>[49]</sup> Another precursor, the colloidal suspension of exfoliated rGO nanosheets was prepared by a chemical reduction of GO using hydrazine.<sup>[50]</sup> The solid-type GO and rGO were obtained by freeze-drying the colloidal suspensions of the nanosheets at  $-45^{\circ}\text{C}$ .

**PEG-L-PA Synthesis:** PEG-L-PA was synthesized by the ring opening polymerization of the N-carboxy anhydrides of L-alanine in the presence of  $\alpha$ -amino- $\omega$ -methoxy PEG.<sup>[25]</sup> The  $\alpha$ -amino- $\omega$ -methoxy PEG (5.0 g, 5.0 mmol; MW 1000 Da) was dissolved in anhydrous toluene (70 mL) and the residual water was removed by azeotropic distillation to a



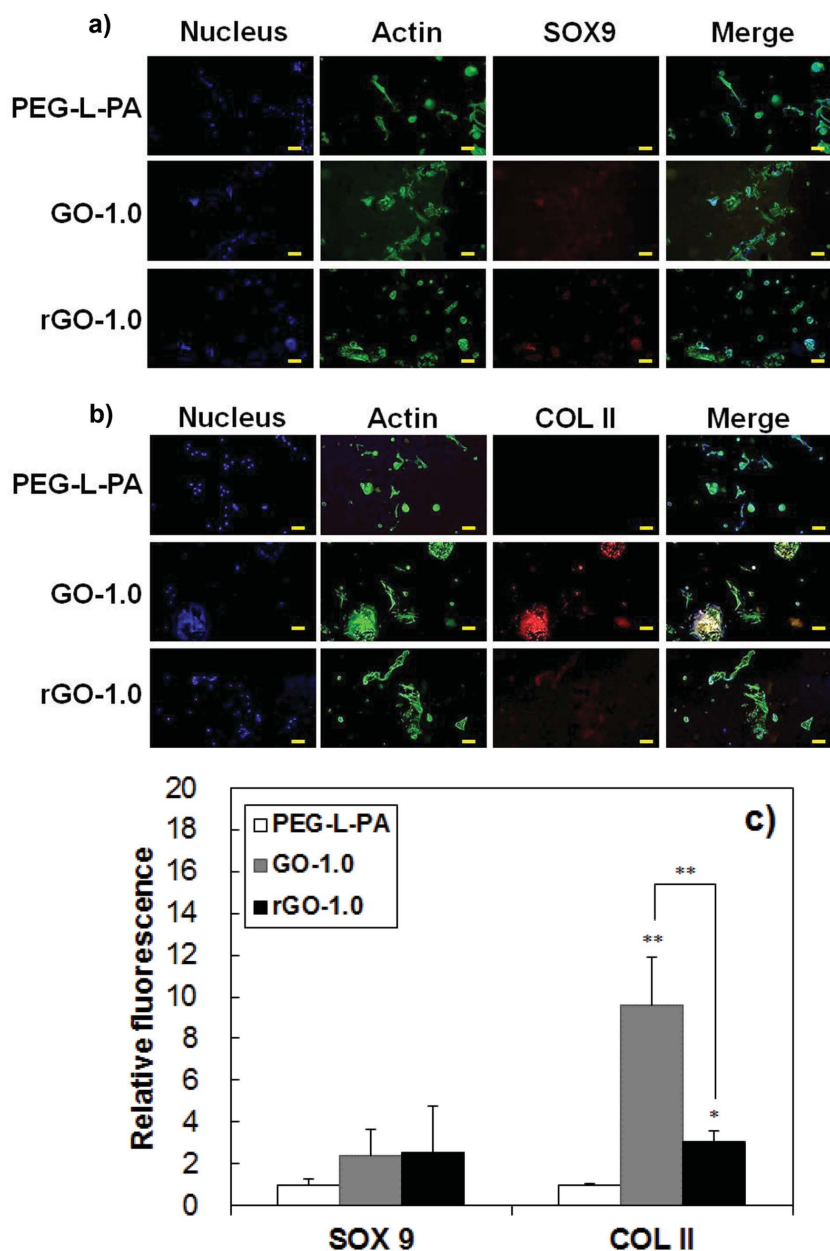


**Figure 8.** Immunofluorescence images for biomarker expressions during TMSC culture in a) the GO/PEG-L-PA hybrid system and b) the rGO/PEG-L-PA hybrid systems using chondrogenic media. c) Semiquantitative treatment of the fluorescence images. The data are presented as the mean  $\pm$  SD of three independent experiments ( $n = 3$ ). The concentration of GO or rGO was fixed at 1.0 wt% in the PEG-L-PA aqueous solution (5.5 wt%). The \* or \*\* on the bar graph indicates the significance of the 2D/3D hybrid system compared with the PEG-L-PA 3D culture system. The scale bar is 50  $\mu$ m.

final volume of about 10 mL. Anhydrous chloroform/*N,N*-dimethyl form amide (40 mL; 2/1 v/v) and *N*-carboxy anhydrides of *L*-alanine (10.2 g, 88.7 mmol) were added to the reaction mixtures. They were stirred at 40  $^{\circ}$ C for 24 h under anhydrous nitrogen conditions. The polymer was purified by repeated dissolution in chloroform, filtration of an undissolved fraction, followed by precipitation into diethyl ether, and then evaporation of the residual solvent under vacuum. The polymer was dialyzed in water using a membrane with a molecular weight cutoff of 1000 Da and freeze-dried. The yield was about 75%.

**$^1$ H-NMR Spectroscopy:**  $^1$ H NMR spectra of PEG-L-PA in  $\text{CF}_3\text{COOD}$  (500 MHz NMR spectrometer; Varian, USA) were used to determine the composition and average molecular weight ( $M_n$ ) of the polymer. In addition,  $^1$ H-NMR spectral changes of the PEG-L-PA aqueous solutions (5.5 wt% in  $\text{D}_2\text{O}$ ) were investigated as a function of temperature in a temperature range of 10–60  $^{\circ}$ C. The solution temperature was equilibrated for 15 min at each temperature before measurements.

**Gel Permeation Chromatography (GPC):** The gel permeation chromatography system (Waters 515) with a refractive index detector (Waters 410) was used to obtain the molecular weights and molecular weight distribution of PEG-L-PA. *N,N*-dimethyl form amide was used as an eluting solvent. Poly(ethylene glycol)s with a molecular weight range of 400–20 000 Da were used as the molecular weight standards. An OHPAK SB-803QH column (Shodex) was used.

**Circular Dichroism (CD) Spectroscopy:** CD spectra of the PEG-L-PA aqueous solution were measured by a CD instrument (J-810, JASCO, Japan) as a function of concentration in a range of 0.001–1.0 wt% at 15  $^{\circ}$ C. In addition, the ellipticity of the PEG-L-PA aqueous solution was obtained as a function of temperature in a range of 10–60  $^{\circ}$ C at a fixed concentration of 0.05 wt% in order to study the change in secondary structure of the polypeptide as a function of temperature. To observe any change in secondary structure of PEG-L-PA by adding GO or rGO, the CD spectra of PEG-L-PA aqueous solution (0.05 wt%) were studied in the presence of GO or rGO.

**Transmission Electron Microscopy (TEM):** The TEM images of GO and rGO were obtained by using a JEM-2100F microscope (JEOL, Japan) with an accelerating voltage of 200 kV.

**Micro-Raman Spectroscopy:** Micro-Raman spectra of the GO and rGO were measured with JY LabRam HR spectrometer using an excitation wavelength of 514.5 nm.

**X-Ray Photoelectron Spectroscopy (XPS):** The XPS machine (Thermo UK) adopted a monochromatic source of Al K-alpha. Any possible shift of the XPS peak caused by the charging effect was calibrated by referencing it to the C1s peak at 284.8 eV.

**Dynamic Mechanical Analysis:** The modulus of the polymer aqueous solution (5.5 wt%) was investigated by dynamic rheometry (Rheometer RS 1; Thermo Haake, Germany) at 4 and 37  $^{\circ}$ C. The aqueous polymer solution was placed between parallel plates with 25 mm in diameter and a gap of 0.5 mm. In addition, the modulus of the in situ formed PEG-L-PA hydrogel containing GO or rGO was investigated at 37  $^{\circ}$ C as a function of GO or rGO concentration. During the dynamic mechanical analysis, the samples were placed inside a chamber with water-soaked cotton to minimize water evaporation. The data were collected

under a controlled stress (4.0 dyn  $\text{cm}^{-2}$ ) and frequency of 1.0 rad  $\text{s}^{-1}$ .

**FTIR Spectroscopy:** The FTIR spectra (FTIR spectrophotometer FTS-800; Varian) of the PEG-L-PA aqueous solution (5.5 wt% in  $\text{D}_2\text{O}$ ) containing GO or rGO (1.0 wt%) were investigated at 37  $^{\circ}$ C.

**TMSC 2D Culture:** TMSCs were isolated from palatine tonsils of 11 years old female donor (IRB approval code: ETC 11-53-02) at the Ewha Womans University Mokdong Hospital (Seoul, Korea) following the ethical guidelines of the University. Briefly, after obtaining the informed consent form from the donor, the tonsils were collected from the patient by tonsillectomy. TMSCs received from Ewha Womans University



**Table 2.** Primer sequences of typical mesodermal differentiation biomarkers and PCR conditions for their real-time RT-PCR. F and R indicate forward and reverse primers, respectively.

Gene	Primer sequences	Annealing temp. [°C]
PPAR $\gamma$	F: 5'-GAAGACGGAGACAGACATGAG-3' R: 5'-GCAACTGGAAGAAGGGAAATG-3'	54.7
COL II	F: 5'-CCCTAACCAAGGATGCACTATG-3' R: 5'-CAGTTCTTGGCTGGGATGTT-3'	55.3
OCN	F: 5'-AGGAGGGAGGTGTGTGAG-3' R: 5'-CTAGACCGGGCCGTAGAA-3'	56.1
GAPDH	F: 5'-CTCCTCACAGTTGCCATGTA-3' R: 5'-GTTGAGCACAGGCTACTTTATTG-3'	54.5

Medical School were cultured in high glucose DMEM containing 10% fetal bovine serum (FBS) (Hyclone, USA) and 1% penicillin/streptomycin (Hyclone, USA) under a 5% CO<sub>2</sub> atmosphere at 37 °C. As a comparative purpose, the TMSCs were 2D cultured (passage 6) on the GO and rGO by using the above growth media. As typical mesodermal differentiation biomarker expression for osteogenesis, chondrogenesis, and adipogenesis, osteocalcin (OCN), type II collagen (COL II), and peroxisome proliferator-activated receptor gamma (PPAR $\gamma$ ) were investigated after the incubation of the cells for 0, 3, 7, and 14 days. Primer sequences of the OCN, COL II, PPAR $\gamma$ , and glyceraldehyde-3-phosphate-dehydrogenase (GAPDH) are shown in **Table 2**.

**TMSC Culture in 2D/3D Hybrid Systems Using Growth Medium:** To prepare 2D/3D hybrid cell culture systems, the harvested TMSCs (passage 6, 0.20  $\times 10^6$  cells) were mixed in a GO or rGO-suspended PEG-L-PA aqueous solution (5.5 wt%, 0.20 mL) and were incubated in 24-well culture plates at 37 °C, during which TMSCs were encapsulated in the GO/PEG-L-PA or rGO/PEG-L-PA gel by the sol-to-gel transition of the polymer aqueous solution. The GO or rGO concentration varied over 0, 0.01, 0.1, and 1.0 wt%. DMEM (2.0 mL) at 37 °C containing 10% FBS and 1% penicillin/streptomycin was added on top of the cell-encapsulated hydrogel and the cells were cultured under a 5% CO<sub>2</sub> atmosphere at 37 °C. The medium was replaced every three days. After 14 days of cell culture, the total RNA content was extracted from the cell-encapsulated hydrogels using the TRIZOL reagent (Invitrogen, USA) according to the manufacturer's protocol. The extracted RNA pellet was dissolved in nuclease-free water, and the RNA quality and concentration were determined using the Experion system (Bio-Rad, USA). After synthesizing the cDNA from the isolated RNA, real-time RT-PCRs were performed with the CFX96 system using the IQ SYBR Green Supermix. The sequence of primers of OCN, COL II, PPAR $\gamma$ , and GAPDH are listed in **Table 2**. The relative expression level of target genes was calculated as  $2^{-\Delta\Delta C_t}$ , where target gene expression was normalized as  $\Delta\Delta C_t = (\text{Gene A} - \text{GAPDH})_t - (\text{Gene A} - \text{GAPDH})_{t_0}$ .  $t_0$  (zero day) indicates on the day when the experiment was started. After 14 days of 3D cell-culture, the cell-encapsulated hydrogels were fixed in natural buffered formalin (NBF). The fixed gels were embedded in an optical-cutting temperature compound (OCT, Sakura, Netherlands) for 12 h, and then they were frozen. The frozen gel samples were then sliced into 10  $\mu\text{m}$  thickness sections at -20 °C and attached to the slide glass. The cryo-sections were stored at -80 °C before staining. For the immunofluorescence study on COL II, the sections embedded in OCT were incubated at 15 °C with aqueous solutions (500  $\mu\text{L}$ /cryo-section) of anti-COL II antibody (Abcam, UK). After washing the section, antibodies were detected using aqueous solutions (500  $\mu\text{L}$ ) of corresponding secondary antibodies (Abcam, UK) according to the manufacturer's protocol. The section was then incubated with DAPI (Molecular Probes, USA) for nucleus staining and phalloidin (Molecular Probes, USA) for actin staining. Labeled cells were then viewed under an Olympus IX71 fluorescence microscope, and the images were captured using Olympus DP2-DSW software.

**Table 3.** Primer sequences of chondrogenic biomarkers and PCR conditions for their real-time RT-PCR. F and R indicate forward and reverse primers, respectively.

Gene	Primer sequences	Annealing temp. [°C]
SOX 9	F: 5'-ACCTTTGGGCTGCCTTATATT-3' R: 5'-TCCCTCACTCCAAGAGAAGAT-3'	54.3
COL II A1	F: 5'-CAAACCCAAAGGACCCAAGTA-3' R: 5'-TGTGAGAGGGTGGGATGAA-3'	55.1
COL II	F: 5'-CCCTAACCAAGGATGCACTATG-3' R: 5'-CAGTTCTTGGCTGGGATGTT-3'	55.3
COL X	F: 5'-ACCCAAGGACTGGAATCTTTAC-3' R: 5'-GCCATTCTTATACAGGCCTACC-3'	54.5
GAPDH	F: 5'-CTCCTCACAGTTGCCATGTA-3' R: 5'-GTTGAGCACAGGCTACTTTATTG-3'	54.5

**TMSC Culture in 2D/3D Hybrid Systems Using Chondrogenic Induction Medium:** The cell culture in 2D/3D hybrid systems was also performed by using chondrogenic induction media prepared by adding  $0.1 \times 10^{-3}$  M dexamethasone (Sigma, MO, USA), 50  $\mu\text{g mL}^{-1}$  ascorbate 2-phosphate (Sigma), 40  $\mu\text{g mL}^{-1}$  L-proline (Sigma), 100  $\mu\text{g mL}^{-1}$  sodium pyruvate (Sigma), 1 $\times$  insulin-transferrin-selenium premix (ITS, Gibco), and 10 ng mL<sup>-1</sup> TGF- $\beta$ 3 (Peprotech, NJ, USA) to the DMEM containing 10% FBS. The 2D/3D hybrid cell culture systems were prepared in the same way. TMSCs (passage 6, 0.20  $\times 10^6$  cells) were mixed in a GO or rGO-suspended PEG-L-PA aqueous solution (5.5 wt%, 0.20 mL) and were incubated in 24-well culture plates at 37 °C, during which TMSCs were encapsulated in the GO/PEG-L-PA or rGO/PEG-L-PA gel by sol-to-gel transition of the polymer aqueous solution. The GO or rGO concentration was fixed at 1.0 wt% in the 2D/3D hybrid system. The 3D system which does not contain GO or rGO was also compared as a control. mRNA expression of chondrogenic biomarkers of SOX 9 transcription factor (SOX 9), type II A1 collagen (COL II A1), COL II, and type X collagen (COL X) were investigated. The primer sequences of the chondrogenic biomarkers are listed in **Table 3**. Immunofluorescence studies using SOX 9 and COL II were also compared.

**Statistical Analysis:** The data were expressed as the mean  $\pm$  standard error of the mean (SEM). The differences in the mean values were evaluated using the one-way ANOVA with Tukey tests. Differences were considered significant when the  $p$  value was less than 0.05 or 0.01 (marked as \* or \*\*), respectively.

## Supporting Information

Supporting Information is available from the Wiley Online Library or from the author.

## Acknowledgements

This work was supported by the National Research Foundation of Korea Grant funded by the Korean Government (Grant Nos. 2012M3A9C6049835 and 2014M3A9B6034223).

Received: January 24, 2015

Revised: February 20, 2015

Published online: March 19, 2015

- [1] J. M. Grichnik, J. A. Burch, R. D. Schulteis, S. Shan, J. Liu, T. L. Darrow, C. E. Vervaert, H. F. Seigler, *J. Invest. Dermatol.* **2006**, 126, 142.

- [2] I. Bozic, M. A. Nowak, *Science* **2013**, 342, 938.
- [3] M. P. Lutolf, P. M. Gilbert, H. M. Blau, *Nature* **2009**, 462, 433.
- [4] W. L. Murphy, T. C. McDevitt, A. J. Engler, *Nat. Mater.* **2014**, 13, 547.
- [5] E. Dawson, G. Mapili, K. Erickson, S. Taqvi, K. Roy, *Adv. Drug Deliv. Rev.* **2008**, 60, 215.
- [6] C. A. Lyssiotis, L. L. Lairson, A. E. Boitano, H. Wurdak, S. Zhu, P. G. Schultz, *Angew. Chem., Int. Ed.* **2011**, 50, 200.
- [7] B. Kim, I. Park, T. Hoshiba, H. Jiang, Y. Choi, T. Akaike, C. Cho, *Prog. Polym. Sci.* **2011**, 36, 238.
- [8] O. F. Zouani, C. Chanseau, B. Brouillaud, R. Bareille, F. Deliane, M. Foulc, A. Mehdi, M. Durrieu, *J. Cell Sci.* **2012**, 125, 1217.
- [9] S. Watari, K. Hayashi, J. A. Wood, P. Russell, P. F. Nealy, C. J. Murphy, D. C. Genetos, *Biomaterials* **2012**, 33, 128.
- [10] A. J. Engler, S. Sen, H. L. Sweeney, D. E. Discher, *Cell* **2006**, 126, 677.
- [11] D. S. W. Benoit, M. P. Schwartz, A. R. Durney, K. S. Anseth, *Nat. Mater.* **2008**, 7, 816.
- [12] P. S. Mathieu, E. G. Loba, *Tissue Eng. Part B* **2012**, 18, 436.
- [13] R. Tuli, S. Tuli, S. Nandi, X. Huang, P. A. Manner, W. J. Hozack, P. A. Manner, K. G. Danielson, R. S. Tuan, *Stem Cells* **2003**, 21, 681.
- [14] H. Baharvand, S. M. Hashemi, S. K. Ashtiani, A. Farrokhi, *Int. J. Dev. Biol.* **2006**, 50, 645.
- [15] L. A. S. Callahan, S. Xie, I. A. Barker, J. Zheng, D. H. Reneker, A. P. Dove, M. L. Becker, *Biomaterials* **2013**, 34, 9089.
- [16] G. T. Christopherson, H. Song, H. Q. Mao, *Biomaterials* **2009**, 30, 556.
- [17] O. W. Petersen, L. Ronnovjessen, A. R. Howlett, M. J. Bissell, *Proc. Natl. Acad. Sci. USA* **1992**, 89, 9064.
- [18] B. G. Choi, M. H. Park, S. H. Cho, M. K. Joo, H. J. Oh, E. H. Kim, K. Park, D. K. Han, B. Jeong, *Biomaterials* **2010**, 31, 9266.
- [19] W. C. Lee, C. H. Lim, H. Shi, L. A. Tang, Y. Wang, C. T. Lim, K. P. Loh, *ACS Nano* **2011**, 5, 7334.
- [20] S. H. Ku, C. B. Park, *Biomaterials* **2013**, 34, 2017.
- [21] H. H. Yoon, S. H. Bhang, T. Kim, T. Yu, T. Hyeon, B. S. Kim, *Adv. Funct. Mater.* **2014**, 24, 6455.
- [22] D. Y. Ko, U. P. Shinde, B. Yeon, B. Jeong, *Prog. Polym. Sci.* **2013**, 38, 672.
- [23] L. Yu, J. Ding, *Chem. Soc. Rev.* **2008**, 37, 1473.
- [24] M. H. Park, Y. Yu, H. J. Moon, D. Y. Ko, H. S. Kim, H. Lee, K. H. Ryu, B. Jeong, *Adv. Healthcare Mater.* **2014**, 3, 1782.
- [25] S. J. Kim, M. H. Park, H. J. Moon, J. H. Park, D. Y. Ko, B. Jeong, *ACS Appl. Mater. Interfaces* **2014**, 6, 17034.
- [26] S. Janjanin, F. Djouad, R. M. Shanti, D. Baksh, K. Gollapudi, D. Prgomet, L. Rackwitz, A. S. Joshi, R. S. Tuan, *Arthritis Res. Ther.* **2008**, 10, R83.
- [27] K. H. Ryu, K. A. Cho, H. S. Park, J. Y. Kim, S. Y. Woo, I. H. Jo, Y. H. Choi, Y. M. Park, S. C. Jung, S. M. Chung, B. O. Choi, H. S. Kim, *Cytotherapy* **2012**, 14, 1193.
- [28] Y. Sakaguchi, I. Sekiya, K. Yagishita, T. Muneta, *Arthritis Rheum.* **2005**, 52, 2521.
- [29] S. Janjanin, F. Djouad, R. M. Shanti, D. Baksh, K. Gollapudi, D. Prgomet, L. Rackwitz, A. S. Joshi, R. S. Tuan, *Arthritis Res. Ther.* **2008**, 10, R83.
- [30] H. S. Kim, S. Y. Woo, K. H. Ryu, K. A. Cho, I. H. Jo, Y. S. Park, *WIPO Patent WO 2013162330 A1*, **2013**.
- [31] M. K. Joo, D. Y. Ko, S. J. Jeong, M. H. Park, U. P. Shinde, B. Jeong, *Soft Matter* **2013**, 9, 8014.
- [32] W. Ding, S. Lin, J. Lin, L. Zhang, *J. Phys. Chem. B* **2008**, 112, 776.
- [33] Y. Y. Choi, M. K. Joo, Y. S. Sohn, B. Jeong, *Soft Matter* **2008**, 4, 2383.
- [34] L. Yu, Z. Zhang, J. Ding, *Biomacromolecules* **2011**, 12, 1290.
- [35] C. Yang, X. Ni, J. Li, *J. Mater. Chem.* **2009**, 19, 3755.
- [36] S. Ahn, E. C. Monge, S. C. Song, *Langmuir* **2009**, 25, 2407.
- [37] A. C. Ferrari, J. Robertson, *Phys. Rev. B* **2000**, 61, 14095.
- [38] D. Pan, S. Wang, B. Zhao, M. Wu, H. Zhang, Y. Wang, Z. Jiao, *Chem. Mater.* **2009**, 21, 3136.
- [39] E. Volkmer, U. Leicht, M. Moritz, C. Schwarz, H. Wiese, S. Milz, P. Matthias, W. Schloegl, W. Friess, M. Coettlinger, P. Augat, M. Schieker, *J. Mater. Sci.: Mater. Med.* **2013**, 24, 2223.
- [40] B. Yeon, M. H. Park, H. J. Moon, S. J. Kim, Y. W. Cheon, B. Jeong, *Biomacromolecules* **2013**, 14, 3256.
- [41] D. Bosnakovski, M. Mizuno, G. Kim, S. Takagi, M. Okumura, T. Fujinaga, *Biotechnol. Bioeng.* **2006**, 93, 1152.
- [42] D. Vivien, P. Galera, E. Lebrun, G. Loyau, J. P. Pujol, *J. Cell Physiol.* **1990**, 143, 534.
- [43] L. Attisano, J. L. Wrana, *Science* **2002**, 296, 1646.
- [44] E. J. Kye, S. J. Kim, M. P. Park, H. J. Moon, K. H. Ryu, B. Jeong, *Biomacromolecules* **2014**, 15, 2180.
- [45] M. H. Park, B. G. Choi, B. Jeong, *Adv. Funct. Mater.* **2012**, 22, 5118.
- [46] M. Motoyama, M. Deie, A. Kanaya, M. Nishimori, A. Miyamoto, S. Yanada, N. Adachi, M. Ochi, *J. Biomed. Mater. Res. A* **2010**, 92, 196.
- [47] H. H. Yoon, S. H. Bhang, J. Y. Shin, J. H. Shin, B. S. Kim, *Tissue Eng.* **2012**, 18, 1949.
- [48] N. R. Gandavarapu, P. D. Mariner, M. P. Wchwartz, K. S. Anseth, *Acta Biomater.* **2013**, 9, 4525.
- [49] D. Li, M. B. Müller, S. Gilje, R. B. Kaner, G. G. Wallace, *Nat. Nanotechnol.* **2008**, 3, 101.
- [50] S. Stankovich, D. A. Dikin, R. D. Piner, K. A. Kohlhaas, A. Kleinhammes, Y. Jia, Y. Wu, S. B. Nguyen, R. S. Ruoff, *Carbon* **2007**, 45, 1558.